

Electron Transfer Between Colloidal ZnO Nanocrystals

Rebecca Hayoun, Kelly M. Whitaker, Daniel R. Gamelin,* and James M. Mayer*

Department of Chemistry, University of Washington, Box 351700, Seattle, Washington 98195-1700, United States

S Supporting Information

ABSTRACT: Colloidal ZnO nanocrystals capped with dodecylamine and dissolved in toluene can be charged photochemically to give stable solutions in which electrons are present in the conduction bands of the nanocrystals. These conduction-band electrons are readily monitored by EPR spectroscopy, with g^* values that correlate with the nanocrystal sizes. Mixing a solution of charged small nanocrystals ($e^-_{\text{CB}}:\text{ZnO}-\text{S}$) with a solution of uncharged large nanocrystals ($\text{ZnO}-\text{L}$) caused changes in the EPR spectrum indicative of quantitative electron transfer from small to large nanocrystals. EPR spectra of the reverse reaction, $e^-_{\text{CB}}:\text{ZnO}-\text{L} + \text{ZnO}-\text{S}$, showed that electrons do not transfer from large to small nanocrystals. Stopped-flow kinetics studies monitoring the change in the UV band-edge absorption showed that reactions of 50 μM nanocrystals were complete within the 5 ms mixing time of the instrument. Similar results were obtained for the reaction of charged nanocrystals with methyl viologen (MV^{2+}). These and related results indicate that the electron-transfer reactions of these colloidal nanocrystals are quantitative and very rapid, despite the presence of ~ 1.5 nm long dodecylamine capping ligands. These soluble ZnO nanocrystals are thus well-defined redox reagents suitable for studies of electron transfer involving semiconductor nanostructures.

Charge-transfer reactions are critical to many applications of nanoscale materials, such as in dye-sensitized solar cells.¹ Interfacial charge transfer is also key to heterogeneous photocatalysis and redox dissolution of minerals in the environment.² Although there has been a great deal of study of electron transfer (ET) involving nanocrystals,³ many aspects remain poorly understood. Zinc oxide (ZnO) has long attracted interest for its electronic, optical, and photochemical properties.⁴ It has also been used to develop a fundamental understanding of interfacial ET in electrochemical cells.⁵ Here, we describe ET reactions involving differently sized colloidal ZnO nanocrystals (quantum dots) that have been photochemically charged. Bimolecular ET between these nanocrystals is quantitative and very rapid. The driving force for ET derives from the greater quantum confinement of the electrons in the smaller nanocrystals. The rapid ET is surprising in light of the ~ 1.5 nm long dodecylamine capping ligands and the common observation of low conductivity in thin films of capped nanocrystals.⁶ These results show that the mixing of nanocrystals in solution is a valuable approach for probing interparticle redox chemistry.

The ZnO and Mn²⁺-doped ZnO nanocrystals investigated here were prepared following reported methods^{7–9} and thereafter treated

as molecular reagents. Their average sizes and size distributions were determined spectroscopically from the energies and shapes of the first excitonic absorption features.¹⁰ The concentrations of nanocrystals were determined from their average size and the total zinc concentration, which was measured using ICP–AES. As reported previously, UV irradiation creates reduced nanocrystals, denoted as $e^-_{\text{CB}}:\text{ZnO}$.¹¹ Charging can be monitored by the appearance of a strong EPR signal^{12–14} and bleaching of the absorption edge in the UV spectrum. Because the reduced nanocrystals are rapidly oxidized by air, all manipulations were performed in a nitrogen-filled glovebox, and EPR spectra were taken in EPR tubes with PTFE valves. Under rigorously anaerobic conditions, the nanocrystals remain charged for weeks without measurable decay¹² and can thus be used as soluble reducing agents in toluene.

The studies reported here involved dodecylamine-capped ZnO nanocrystals of two different diameters (3.7 ± 0.2 and 6.0 ± 2.0 nm), termed $\text{ZnO}-\text{S}$ and $\text{ZnO}-\text{L}$ for small and large, respectively.⁹ Brief irradiation yielded nanocrystal solutions that exhibited EPR resonances with $g^* = 1.967$ for $e^-_{\text{CB}}:\text{ZnO}-\text{S}$ and 1.963 for $e^-_{\text{CB}}:\text{ZnO}-\text{L}$ [Figure 1a; the signals at $g^* = 2.0037$ are from the external calibration standard 2,2-diphenyl-1-picrylhydrazyl radical (DPPH)]. The observed size dependence of the g^* values is one of the indications that the added electron is delocalized in the conduction band (CB) and not localized in a trap site, as discussed previously.^{12–14} For a given sample and with short irradiation times, g^* did not vary with charging time. This result indicates that the nanocrystals have fewer than one electron each on average ($\langle n_e \rangle < 1$).¹³

The size dependence of the $e^-_{\text{CB}}:\text{ZnO}$ EPR signal provides a direct way to monitor ET between nanocrystals. A 0.5 mL solution of small nanocrystals (1×10^{-4} M, where M denotes moles of nanocrystals per liter) was irradiated to form $e^-_{\text{CB}}:\text{ZnO}-\text{S}$, and an EPR spectrum was taken. This solution was then mixed with 0.5 mL of an equimolar solution of uncharged $\text{ZnO}-\text{L}$. The EPR spectrum of the mixed solution showed a signal at $g^* = 1.963$ characteristic of $e^-_{\text{CB}}:\text{ZnO}-\text{L}$ rather than the signal of the starting small nanocrystals at $g^* = 1.967$ (Figure 1b, dashed). This shift in g^* shows that the CB electrons were transferred from the small nanocrystals to the larger ones (Scheme 1). Reaction in the reverse direction, examined by mixing $e^-_{\text{CB}}:\text{ZnO}-\text{L}$ with $\text{ZnO}-\text{S}$, showed no change in g^* before and after mixing (Figure 1c). This result shows that electrons are not transferred from large to small nanocrystals.

The driving force for ET from small to large nanocrystals comes from quantum confinement. The band gap is larger in the smaller particles, as is evident from the optical spectra, and the shifts in the individual valence and conduction bands (HOMO

Received: December 10, 2010

Published: March 08, 2011

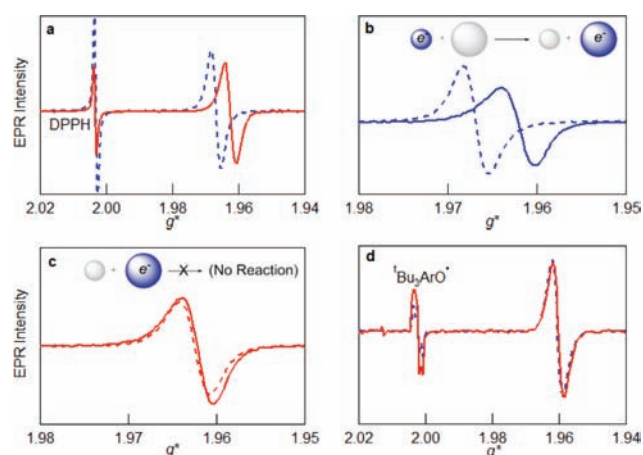
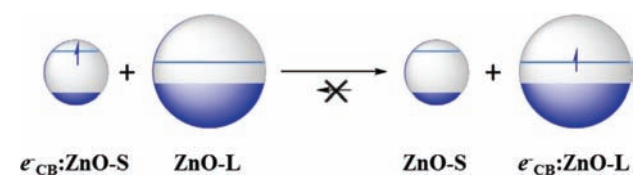


Figure 1. EPR spectra of $e^-_{\text{CB}}:\text{ZnO}$ nanocrystals in toluene at 298 K. (a) Spectra of $e^-_{\text{CB}}:\text{ZnO-S}$ (blue dashed line) and $e^-_{\text{CB}}:\text{ZnO-L}$ (red solid line), with DPPH as an external standard, showing the dependence of g^* on nanocrystal size. (b) Spectra of $e^-_{\text{CB}}:\text{ZnO-S}$ (dashed) and the reaction mixture $e^-_{\text{CB}}:\text{ZnO-S} + \text{ZnO-L}$ (solid), showing the transfer of electrons to ZnO-L . (c) Spectra of $e^-_{\text{CB}}:\text{ZnO-L}$ (dashed) and mixed $e^-_{\text{CB}}:\text{ZnO-L} + \text{ZnO-S}$ (solid), showing no transfer of electrons. (d) Spectra of $e^-_{\text{CB}}:\text{ZnO-L}$ (blue dashed) and mixed $e^-_{\text{CB}}:\text{ZnO-L} + \text{ZnO-L}$ (red solid), with a capillary of $t\text{Bu}_3\text{ArO}^\bullet$ as a standard, showing negligible loss of EPR intensity upon mixing. In (b–d), the intensities of the spectra of the mixed solutions have been doubled to account for dilution.

Scheme 1



and LUMO) can be estimated from the Brus equation.^{15,16} The CB energy for ZnO-S was estimated to be 0.21 eV higher than that for ZnO-L .⁹ With the assumption that this energy difference equals the difference in redox potentials, an equilibrium constant $K_{\text{eq}} = 10^{3.5}$ at room temperature is predicted, consistent with the experimental observation of complete transfer from small to large nanocrystals.¹⁷

Reduced nanocrystals were also mixed with uncharged nanocrystals of the same size from the same synthetic batch. EPR spectra of $e^-_{\text{CB}}:\text{ZnO-S}$ before and after mixing with an equal portion of uncharged ZnO-S showed no shift in g^* . The same behavior was observed for $e^-_{\text{CB}}:\text{ZnO-L} + \text{ZnO-L}$. These results confirmed that the shift in g^* in Figure 1b was due only to transfer of electrons from ZnO-S to ZnO-L , and not, for example, to a decrease in $\langle n_e \rangle$,¹³ trap filling, or some sort of aggregation behavior.

To quantitatively monitor the number of unpaired spins in a reaction, the double-integrated $e^-_{\text{CB}}:\text{ZnO}$ EPR intensities were compared with that of an internal capillary standard of 2,4,6-tri-*tert*-butylphenoxy radical ($t\text{Bu}_3\text{ArO}^\bullet$).^{9,18} A portion of a ZnO-L solution was irradiated, and the intensity of the $e^-_{\text{CB}}:\text{ZnO}$ EPR resonance was determined versus the standard. An equal amount of the same ZnO-L solution that had not been charged was added to this EPR tube, and another spectrum was recorded



Figure 2. (a) EPR spectra of $e^-_{\text{CB}}:\text{ZnO-S}$ (top, red), uncharged $\text{Mn}^{2+}:\text{ZnO-L}$ (middle, blue), and mixed $e^-_{\text{CB}}:\text{ZnO-S} + \text{Mn}^{2+}:\text{ZnO-L}$ (bottom, black). (b) EPR spectra of $e^-_{\text{CB}}:\text{ZnO-L}$ (top, red), uncharged $\text{Mn}^{2+}:\text{ZnO-S}$ (middle, blue), and mixed uncharged $\text{Mn}^{2+}:\text{ZnO-S} + e^-_{\text{CB}}:\text{ZnO-L}$ (bottom, black). The sharp signal for $e^-_{\text{CB}}:\text{ZnO-L}$ was unchanged.

(Figure 1d). As found above, the g^* value did not shift. The double-integrated intensity of the EPR signal after mixing was found to be 48% of the original intensity, the decrease resulting primarily from the 2-fold dilution of the sample. After dilution was taken into account, only $\sim 4\%$ of the original EPR intensity was lost upon mixing. (In Figure 1b–d, the intensities of the product spectra have been doubled to account for dilution.) In a similar experiment, $e^-_{\text{CB}}:\text{ZnO-L}$ in toluene was mixed with an equal volume of a 5-fold more dilute solution of ZnO-L in toluene, and again only a small (1%) decrease in intensity was observed after correction for dilution. These small decreases in EPR intensity likely resulted simply from losses associated with handling the dilute and highly air-sensitive solutions. These experiments show that ET occurs between 1S_e CB states with negligible loss to trap states. The role such electron traps might play in ZnO nanocrystal CB filling has been debated in the recent literature.¹⁹

Another probe of ET is provided by Mn^{2+} -doped ZnO nanocrystals, which show a characteristic multiline EPR signal (hyperfine constant $A_{\text{iso}} \approx 74 \times 10^{-4} \text{ cm}^{-1}$; Figure 2a,b, middle spectra).⁸ EPR spectra of reduced $\text{Mn}^{2+}:\text{ZnO}$ nanocrystals do not show a simple derivative signal like that in Figure 1; instead, they show broadening of the Mn^{2+} multiline signal due to $e^-_{\text{CB}}-\text{Mn}^{2+}$ exchange coupling.^{12,20} A solution of uncharged $\text{Mn}^{2+}:\text{ZnO-L}$ ($\sim 0.7\% \text{ Mn}^{2+}$) was mixed with a 10-fold excess of $e^-_{\text{CB}}:\text{ZnO-S}$. The EPR spectra of the reaction solution showed loss of the sharp signal for the $e^-_{\text{CB}}:\text{ZnO-S}$ CB electron and a broadening of the Mn^{2+} fine structure (Figure 2a, bottom spectrum).⁹ To see significant broadening, an excess of $e^-_{\text{CB}}:\text{ZnO-S}$ was used, and these nanocrystals were more extensively photochemically charged.⁹ The inverse reaction, involving mixing of $e^-_{\text{CB}}:\text{ZnO-L}$ with $\text{Mn}^{2+}:\text{ZnO-S}$, gave an EPR spectrum with a superposition of the unbroadened Mn^{2+} multiplet and the sharp e^-_{CB} resonance (Figure 2b). These results support the conclusion that electrons are readily transferred from small to large nanocrystals but not in the reverse direction.

The ET kinetics were examined by optical spectroscopy using a stopped-flow apparatus.⁹ In initial experiments, methyl viologen (MV^{2+}) dichloride was used as the oxidant because its one-electron-reduced form, the radical cation $\text{MV}^{\bullet+}$, has a distinct absorbance at $\lambda_{\text{max}} = 609 \text{ nm}$ ²¹ that is well-separated from the absorbances of ZnO and MV^{2+} . Toluene solutions of $e^-_{\text{CB}}:\text{ZnO-S}$ ($5 \times 10^{-5} \text{ M}$) were rapidly mixed with equimolar solutions of MV^{2+} in 4:1 toluene/ethanol. The first optical spectrum was obtained within 5 ms of mixing and already showed the strong characteristic 609 nm absorbance of $\text{MV}^{\bullet+}$ (Figure 3a). Subsequent

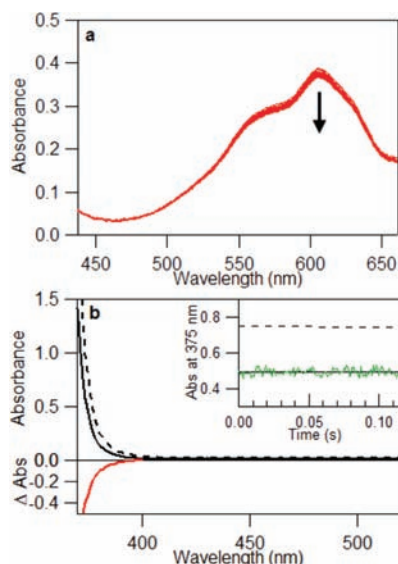


Figure 3. (a) Selected optical spectra for the reaction between 5×10^{-5} M MV^{2+} and $e^-_{CB}:ZnO$. The top spectrum was obtained within 5 ms after mixing, and the subsequent spectra were recorded at intervals of 150 ms. (b) Experimental spectrum of $e^-_{CB}:ZnO-S + ZnO-L$ in toluene 5 ms after mixing (solid black line) compared with the sum of the separate spectra for $e^-_{CB}:ZnO-S$ and $ZnO-L$ (corrected for dilution, dashed black line). The difference spectrum (exptl - calcd; red line) shows the band-edge bleaching. Inset: Experimental absorbance at 375 nm vs time and a linear fit (solid line); the dashed line indicates A_{375} calculated for a hypothetical unreacted mixture of $e^-_{CB}:ZnO-S + ZnO-L$.

spectra were almost identical, showing only slow decay of the MV^{*+} intensity over seconds, likely due to the presence of adventitious oxygen.²² This result demonstrates rapid ET from reduced ZnO to MV^{2+} , forming MV^{*+} .

With the same stopped-flow apparatus, 5×10^{-5} M solutions of $e^-_{CB}:ZnO-S$ were rapidly mixed with an equivalent amount of $ZnO-L$. Again, the optical spectra were essentially constant from the first spectrum ~ 5 ms after mixing. The resulting spectrum is shown as the solid black line in Figure 3b. The dashed black line shows the spectrum anticipated for the $e^-_{CB}:ZnO-S + ZnO-L$ mixture had no reaction occurred, as obtained by mathematically adding the separately measured spectra of these two solutions. The absorbance change upon mixing was small, but the difference spectrum (red, bottom) clearly showed bleaching at the band edge (~ 375 nm) that is consistent with ET from small to large nanocrystals.

In the reactions of $e^-_{CB}:ZnO-S$ with MV^{2+} and $e^-_{CB}:ZnO-S$ with $ZnO-L$, the optical spectra showed complete reaction of the $50 \mu M$ solutions within 5 ms. With the assumption of second-order kinetics, this implies bimolecular rate constants of $>10^7 M^{-1} s^{-1}$. These are remarkably large rate constants, within 3 orders of magnitude of the diffusion limit.⁹ The very rapid ET between the nanocrystals is surprising because each particle was capped by ~ 1.5 nm long dodecylamine ligands. If the capping groups form a ~ 3 nm dielectric tunneling barrier for interparticle ET, the largest possible rate constant would be $\sim 10 M^{-1} s^{-1}$ (when $\Delta G^\circ = -\lambda$ and taking $k^0 = 10^{14} s^{-1}$ and $\beta = 1 \text{ \AA}^{-1}$).²³ This kind of barrier has been invoked to explain the low conductivities of thin films of capped semiconducting nanoparticles.⁶ Closer approach of the ZnO nanocrystals may be possible because of incomplete capping or interpenetration of the dodecylamine chains from different particles.

Indeed, ligand interdigitation has been proposed to explain rapid interparticle ET in films of thiolate-capped gold clusters.²⁴ A rate constant of $10^7 M^{-1} s^{-1}$ could be consistent with a 1.5 nm particle separation, but just barely.

In conclusion, EPR and optical spectra demonstrate rapid ET between colloidal dodecylamine-capped ZnO nanocrystals in toluene. Electrons in the conduction bands of 3.7 ± 0.2 nm diameter nanocrystals were readily transferred to the conduction bands of 6.0 ± 2.0 nm diameter nanocrystals, but no ET occurred in the opposite direction. The quantitative ET from small to large nanocrystals is consistent with the band-edge energies anticipated from the Brus equation.¹⁵ Integration of the EPR spectra showed that the ET is quantitative and that there are no significant EPR-silent trap states. Stopped-flow optical experiments indicated that the ET occurs very rapidly, with apparent bimolecular rate constants of $>10^7 M^{-1} s^{-1}$. This simple and direct method of mixing charged nanocrystals in solution has thus provided new insights into nanoscale ET processes. Experiments using this approach to probe the roles of capping ligands, counterions, solvent, and the number of electrons per nanocrystal in interparticle ET reactions are underway.

■ ASSOCIATED CONTENT

S Supporting Information. Experimental details and additional spectra. This material is available free of charge via the Internet at <http://pubs.acs.org>.

■ AUTHOR INFORMATION

Corresponding Author

gamelin@chem.washington.edu; mayer@chem.washington.edu

■ ACKNOWLEDGMENT

We are grateful to the University of Washington for financial support to J.M.M., R.H., and K.M.W. and to the U.S. National Science Foundation (CHE 0628252-CRC) for support for D.R. G. and K.M.W. EPR instrumentation support was provided by the Center for Ecogenetics and Environmental Health (UW Center Grant P30 ES07033 from the National Institute of Environmental Health Sciences). We thank Drs. Stefan T. Ochsnein and Kevin R. Kittilstved for helpful discussions.

■ REFERENCES

- (1) (a) O'Regan, B.; Grätzel, M. *Nature* **1991**, *353*, 737–740. (b) Grätzel, M. *Nature* **2001**, *414*, 338–344. (c) Hagfeldt, A.; Boschloo, G.; Sun, L.; Kloo, L.; Pettersson, H. *Chem. Rev.* **2010**, *110*, 6595–6663.
- (2) (a) Beverskog, B.; Puigdomenech, I. *Corros. Sci.* **1997**, *39*, 107–114. (b) Stumm, W.; Morgan, J. J. *Aquatic Chemistry*, 3rd ed.; Wiley-Interscience: New York, 1996. (c) Thompson, T. L.; Yates, J. T., Jr. *Chem. Rev.* **2006**, *106*, 4428–4453.
- (3) (a) Meulenlamp, E. A. *J. Phys. Chem. B* **1999**, *103*, 7831–7838. (b) Biju, V.; Micic, M.; Hu, D.; Lu, H. P. *J. Am. Chem. Soc.* **2004**, *126*, 9374–9381. (c) Robel, I.; Subramanian, V.; Kuno, M.; Kamat, P. V. *J. Am. Chem. Soc.* **2006**, *128*, 2385–2393. (d) Boulesbaa, A.; Issac, A.; Stockwell, D.; Huang, Z.; Huang, J.; Guo, J.; Lian, T. *J. Am. Chem. Soc.* **2007**, *129*, 15132–15133. (e) Gocalińska, A.; Saba, M.; Quochi, F.; Marceddu, M.; Szendrei, K.; Gao, J.; Loi, M. A.; Yarema, M.; Seyrkammer, R.; Heiss, W.; Mura, A.; Bongiovanni, G. *J. Phys. Chem. Lett.* **2010**, *1*, 1149–1154.
- (4) (a) Look, D. C. *Mater. Sci. Eng., B* **2001**, *80*, 383–387. (b) Klingshirn, C. *ChemPhysChem* **2007**, *8*, 782–803.

- (5) Hamann, T. W.; Gstrein, F.; Brunschwig, B. S.; Lewis, N. S. *Chem. Phys.* **2006**, 326, 15–23.
- (6) Talapin, D. V.; Lee, J.-S.; Kovalenko, M. V.; Shevchenko, E. V. *Chem. Rev.* **2010**, 110, 389–458. See Table 1 on p 402.
- (7) Schwartz, D. A.; Norberg, N. S.; Nguyen, Q. P.; Parker, J. M.; Gamelin, D. R. *J. Am. Chem. Soc.* **2003**, 125, 13205–13218.
- (8) Norberg, N. S.; Kittilstved, K. R.; Amonette, J. E.; Kukkadapu, R. K.; Schwartz, D. A.; Gamelin, D. R. *J. Am. Chem. Soc.* **2004**, 126, 9387–9398.
- (9) See the Supporting Information.
- (10) (a) Meulenkamp, E. A. *J. Phys. Chem. B* **1998**, 102, 5566–5572. (b) Pesika, N. S.; Stebe, K. J.; Searson, P. C. *Adv. Mater.* **2003**, 15, 1289–1291.
- (11) (a) Haase, M.; Weller, H.; Henglein, A. *J. Phys. Chem.* **1988**, 92, 482–487. (b) Shim, M.; Guyot-Sionnest, P. *J. Am. Chem. Soc.* **2001**, 123, 11651–11654. (c) Reduced particles are formed by quenching of photogenerated holes, presumably by one of the organic compounds in the solution (dodecylamine, ethanol, toluene). The nature of this process is currently under study.
- (12) Liu, W. K.; Whitaker, K. M.; Kittilstved, K. R.; Gamelin, D. R. *J. Am. Chem. Soc.* **2006**, 128, 3910–3911.
- (13) Liu, W. K.; Whitaker, K. M.; Smith, A. L.; Kittilstved, K. R.; Robinson, B. H.; Gamelin, D. R. *Phys. Rev. Lett.* **2007**, 98, No. 186804.
- (14) Whitaker, K. M.; Ochsenbein, S. T.; Polinger, V. Z.; Gamelin, D. R. *J. Phys. Chem. C* **2008**, 112, 14331–14335.
- (15) (a) Brus, L. E. *J. Phys. Chem.* **1986**, 90, 2555–2560. (b) Brus, L. E. *J. Chem. Phys.* **1983**, 79, 5566–5571. (c) Suyver, J. F.; van der Beek, T.; Wuister, S. F.; Kelly, J. J.; Meijerink, A. *Appl. Phys. Lett.* **2001**, 79, 4222–4224.
- (16) (a) This calculation used the effective masses of the electron and hole, which were taken to be those of bulk ZnO.^{16b} (b) Madelung, O. *Semiconductors: Data Handbook*, 3rd ed.; Springer: New York, 2004.
- (17) The use of particle size to modulate electron and energy transfer has been discussed previously. For instance, see: (a) Haram, S. K.; Quinn, B. M.; Bard, A. J. *J. Am. Chem. Soc.* **2001**, 123, 8860–8861. (b) Huss, A. S.; Bierbaum, A.; Chitta, R.; Ceckanowicz, D. J.; Mann, K. R.; Gladfelter, W. L.; Blank, D. A. *J. Am. Chem. Soc.* **2010**, 132, 13963–13965. (c) Kagan, C. R.; Murray, C. B.; Nirmal, M.; Bawendi, M. G. *Phys. Rev. Lett.* **1996**, 76, 1517–1520.
- (18) Manner, V. W.; Markle, T. F.; Freudenthal, J. H.; Roth, J. P.; Mayer, J. M. *Chem. Commun.* **2008**, 256–258.
- (19) (a) Shim, M.; Guyot-Sionnest, P. *Phys. Rev. Lett.* **2003**, 91, No. 169703. (b) Vanmaekelbergh, D.; Roest, A. L.; Germeau, A.; Kelly, J. J.; Meulenkamp, E. A.; Allan, G.; Delerue, C. *Phys. Rev. Lett.* **2003**, 91, No. 169704.
- (20) Ochsenbein, S. T.; Feng, Y.; Whitaker, K. M.; Badaeva, E.; Liu, W. K.; Li, X.; Gamelin, D. R. *Nat. Nanotechnol.* **2009**, 4, 681–687.
- (21) Bockman, T. M.; Kochi, J. K. *J. Org. Chem.* **1990**, 55, 4127–4135.
- (22) In support of this interpretation, over the course of multiple stopped-flow runs with the same set of solutions, this decay became less evident, presumably because the trace O₂ was being flushed from the system.
- (23) (a) Edwards, P. P.; Gray, H. B.; Lodge, M. T. J.; Williams, R. J. P. *Angew. Chem., Int. Ed.* **2008**, 47, 6758–6765. (b) This calculation assumed $K_{\text{eq}} = 1 \text{ M}^{-1}$ for the interparticle precursor complex in order to convert bimolecular and unimolecular ET rate constants.
- (24) Wuelfing, W. P.; Green, S. J.; Pietron, J. J.; Cliffl, D. E.; Murray, R. W. *J. Am. Chem. Soc.* **2000**, 122, 11465–11472.